Identification and biochemical characterization of two novel UDP-2,3-diacetamido-2,3-dideoxy-α-D-glucuronic acid 2-epimerases from respiratory pathogens

Erin L. WESTMAN*, David J. MCNALLY†, Martin REJZEK‡[1], Wayne L. MILLER*, Vellupillai Sri KANNATHASAN§, Andrew PRESTON*, Duncan J. MASKELL||, Robert A. FIELD‡[1], Jean-Robert BRISSON† and Joseph S. LAM*[2]

*Department of Molecular and Cellular Biology, University of Guelph, Guelph, ON, Canada, N1G 2W1, †Institute for Biological Sciences, National Research Council, Ottawa, ON, Canada, K1A 0R6, ‡Centre for Carbohydrate Chemistry, School of Chemical Sciences and Pharmacy, University of East Anglia, Norwich, NR4 7TJ, U.K., §Centre for Carbohydrate Chemistry, School of Chemical Sciences, University of East Anglia, Norwich NR4 7TJ, U.K., and ||Department of Veterinary Medicine, University of Cambridge, Madingley Road, Cambridge CB3 0ES, U.K.

The heteropolymeric O-antigen of the lipopolysaccharide from *Pseudomonas aeruginosa* serogroup O5 as well as the band-A trisaccharide from *Bordetella pertussis* contain the di-N-acetylated mannosaminuronic acid derivative, β-D-ManNAc3NAcA (2,3-diacetamido-2,3-dideoxy-β-D-mannuronic acid). The biosynthesis of the precursor for this sugar is proposed to require five steps, through which UDP-α-D-GlcNAc (UDP-*N*-acetyl-α-D-glucosamine) is converted via four steps into UDP-α-D-GlcNAc3NAcA (UDP-2,3-diacetamido-2,3-dideoxy-α-D-glucuronic acid), and this intermediate compound is then epimerized by WbpI (*P. aeruginosa)*, or by its orthologue, WlbD (*B. pertussis*), to form UDP-α-D-ManNAc3NAcA (UDP-2,3-diacetamido-2,3-dideoxy-α-D-mannuronic acid). UDP-α-D-GlcNAc3NAcA, the proposed substrate for WbpI and WlbD, was obtained through chemical synthesis. His_6–WbpI and His_6–WlbD were overexpressed and then purified by affinity chromatography using FPLC. Capillary electrophoresis was used to analyse reactions with each enzyme, and revealed that both enzymes used UDP-α-D-GlcNAc3NAcA as a substrate, and reacted optimally in sodium phosphate buffer (pH 6.0). Neither enzyme utilized UDP-α-D-GlcNAc, UDP-α-D-GlcNAcA (UDP-2-acetamido-2,3-dideoxy-α-D-glucuronic acid) or UDP-α-D-GlcNAc3NAc (UDP-2,3-diacetamido-2,3-dideoxy-α-D-glucose) as substrates. His_6–WbpI or His_6–WlbD reactions with UDP-α-D-GlcNAc3NAcA produce a novel peak with an identical retention time, as shown by capillary electrophoresis. To unambiguously characterize the reaction product, enzyme–substrate reactions were allowed to proceed directly in the NMR tube and conversion of substrate into product was monitored over time through the acquisition of a proton spectrum at regular intervals. Data collected from one- and two-dimensional NMR experiments showed that His_6–WbpI catalysed the 2-epimerization of UDP-α-D-GlcNAc3NAcA, converting it into UDP-α-D-ManNAc3NAcA. Collectively, these results provide evidence that WbpI and WlbD are UDP-2,3-diacetamido-2,3-dideoxy-α-D-glucuronic acid 2-epimerases.

Key words: 2-epimerase, lipopolysaccharide, mannosaminuronic acid biosynthesis, O antigen, sugar–nucleotide metabolism, UDP-2,3-diacetamido-2,3-dideoxy-α-D-glucuronic acid.

INTRODUCTION

Pseudomonas aeruginosa and *Bordetella pertussis* are important respiratory pathogens in humans. *P. aeruginosa* is an opportunistic pathogen that frequently infects cystic fibrosis patients; *B. pertussis* is a strict human pathogen, being the causative agent of whooping cough. The LPS (lipopolysaccharide) of both organisms contain a di-N-acetylated mannosaminuronic acid residue: β-D-ManNAc3NAcA (2,3-diacetamido-2,3-dideoxy-β-D-mannuronic acid). In *B. pertussis*, β-D-ManNAc3NAcA is found in the band-A trisaccharide, and mutants lacking band A are deficient in nasal colonization in a BALB/c mouse model [1]. In *P. aeruginosa* strain PAO1 (serotype O5), the B-band O-antigen trisaccharide repeat unit contains β-D-ManNAc3NAcA, and is involved in protecting *P. aeruginosa* from serum-mediated killing [2], and from phagocytosis by human polymorphonuclear leucocytes [3]. In both bacteria, β-D-ManNAc3NAcA is suggested to be incorporated into the LPS by the action of an inverting glycosyltransferase that utilizes UDP-α-D-ManNAc3NAcA (UDP-2,3-diacetamido-2,3-dideoxy-α-D-mannuronic acid) and the nascent LPS molecule. Deciphering the biosynthesis of the complex sugar–nucleotide UDP-α-D-ManNAc3NAcA is fundamentally important for understanding how surface polysaccharide layers are made in these respiratory pathogens. In addition, it is interesting to note that the biosynthesis of this sugar–nucleotide occurs through a dedicated pathway that is distinct from that found in other species that produce N-acetylated uronic acid sugars.

α-D-ManNAcA (*N*-acetyl-D-mannosaminuronic acid) is a constituent of both the enterobacterial common antigen of *Escherichia coli* and the polysaccharide capsule of *Staphylococcus aureus*. In these organisms, UDP-α-D-ManNAcA is synthesized from UDP-α-D-GlcNAc (UDP-*N*-acetyl-α-D-glucosamine) via a two-step pathway. In the first step, WecB (formerly RffE; *E. coli*) or Cap5P (*S. aureus*) catalyse a C2 epimerization to form UDP-α-D-ManNAc (UDP-*N*-acetyl-α-D-mannosamine), and in the second step, WecC (formerly RffD; *E. coli*) or Cap5O (*S. aureus*)

Abbreviations used: CE, capillary electrophoresis; α-D-GlcNAc, *N*-acetyl-α-D-glucosamine; α-D-GlcNAcA, 2-acetamido-2,3-dideoxy-α-D-glucuronic acid; α-D-GlcNAc3NAc, 2,3-diacetamido-2,3-dideoxy-α-D-glucose; α-D-GlcNAc3NAcA, 2,3-diacetamido-2,3-dideoxy-α-D-glucuronic acid; HMBC, heteronuclear multiple bond correlation; HSQC, heteronuclear single-quantum coherence; IPTG, isopropyl-thio-β-D-galactopyranoside; LB, Luria–Bertani; LPS, lipopolysaccharide; α-D-ManNAc, *N*-acetyl-α-D-mannosamine; α-D-ManNAcA, *N*-acetyl-D-mannosaminuronic acid; α-D-ManNAc3NAcA, 2,3-diacetamido-2,3-dideoxy-α-D-mannuronic acid; β-D-ManNAc3NAcA, 2,3-diacetamido-2,3-dideoxy-β-D-mannuronic acid.

[1] Present address: Department of Biological Chemistry, John Innes Centre, Colney Lane, Norwich NR4 7UH, U.K.
[2] To whom correspondence should be addressed (email jlam@uoguelph.ca).

catalyse a C6 dehydrogenation to form UDP-α-D-ManNAcA [4–6]. Although it was initially thought that biosynthesis of the mannosaminuronic acid-derived residues of *P. aeruginosa* and *B. pertussis* would follow a similar pathway to that of UDP-α-D-ManNAcA, evidence has accumulated that shows otherwise.

The B-band LPS gene cluster of *P. aeruginosa* contains several loci that are essential for the production of O-antigen [7,8]. These genes include *wbp*A and *wbp*I. WbpI shares more than 50 % similarity with WecB and Cap5P, and was proposed to act as a C2 epimerase on UDP-α-D-GlcNAc [7]. WbpA, which shares greater than 51 % similarity to WecC and Cap5O, was predicted to be a UDP-mannose dehydrogenase and is suggested to act later in the pathway [9]. However, attempts to cross-complement *wecB* and *wbpI*, as well as *wecC* and *wbpA*, were not successful, which indicates that these genes are not functionally interchangeable *in vivo* [9]. In a subsequent study, our group showed that WbpA catalyses the dehydrogenation of UDP-α-D-GlcNAc to form UDP-α-D-GlcNAcA (UDP-2-acetamido-2,3-dideoxy-α-D-glucuronic acid) [10]. Thus the pathway for the biosynthesis of UDP-α-D-ManNAc3NAcA in *P. aeruginosa* is clearly different from the pathway for the biosynthesis of UDP-α-D-ManNAcA in *E. coli* and *S. aureus*. Although both pathways require an epimerase and a dehydrogenase, the enzymes in each of these pathways apparently have different substrate specificities and act at different steps in these systems.

In *B. pertussis*, the metabolic pathway for converting UDP-α-D-GlcNAc into UDP-α-D-ManNAc3NAcA has been proposed to require four steps [11] involving the sequential action of the *wlbA–D* genes found within the *B. pertussis wlb* locus (formerly the *bpl* locus). WlbD, which is 70 % similar to WbpI of *P. aeruginosa*, was proposed to epimerize UDP-α-D-GlcNAc to UDP-α-D-ManNAc. *B. pertussis wlbD*-null mutants produce LPS devoid of the band A trisaccharide [12]. However, no biochemical data have been obtained to establish the function of the WlbA–D proteins.

In the present study, a revised pathway for the production of UDP-α-D-ManNAc3NAcA in *P. aeruginosa* and *B. pertussis* is proposed and the C2 epimerase from each species is characterized. The new pathway proposal is based on biochemical evidence that WbpA utilizes UDP-α-D-GlcNAc as a specific substrate in a dehydrogenation reaction yielding UDP-α-D-GlcNAcA [10], as well as homology-based assignments. UDP-α-D-GlcNAcA is thought to be successively oxidized by WbpB/WlbA, transaminated by WbpE/WlbC, and N-acetylated by WbpD/WlbB, before epimerization to the mannose-derivative form by WbpI/WlbD (Figure 1). We sought to determine the enzymatic activities of WbpI and WlbD from *P. aeruginosa* and *B. pertussis* respectively, in order to test the hypothesis that these proteins are 2-epimerases. M. Rejzek and R.A. Field (unpublished work) recently achieved the chemical synthesis of the di-N-acetylated uronic acid compound, UDP-α-D-GlcNAc3NAcA (UDP-2,3-diacetamido-2,3-dideoxy-α-D-glucuronic acid), proposed to be the substrate for WbpI and WlbD, which provided an opportunity to study these enzymes *in vitro*. Evidence from CE (capillary electrophoresis) and NMR studies demonstrated that WbpI and WlbD are UDP-α-D-ManNAc3NAcA 2-epimerases.

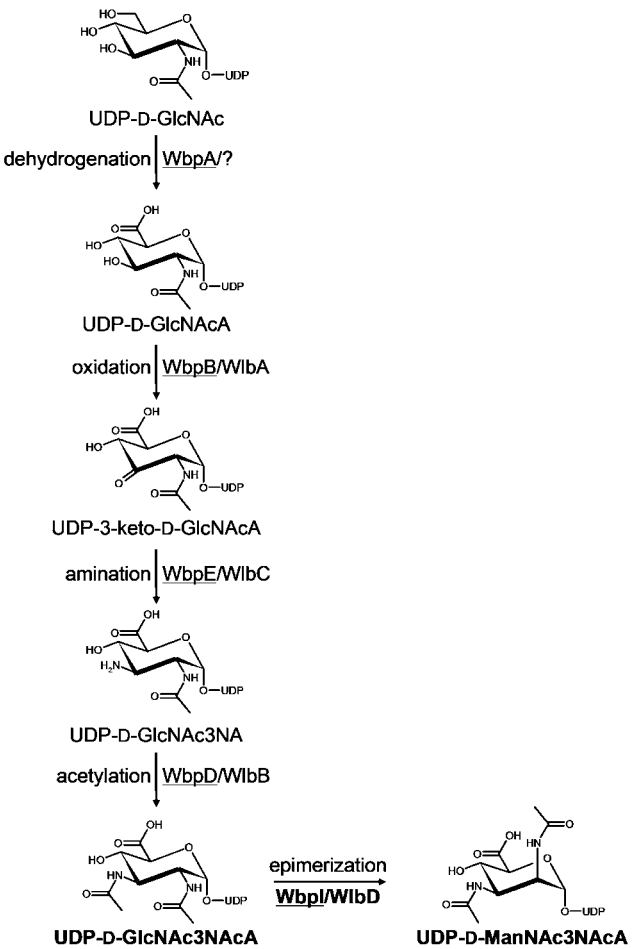

Figure 1 Proposed pathway for the biosynthesis of UDP-D-Man(2NAc3NAc)A in *P. aeruginosa* PAO1 (underlined enzyme names) and *B. pertussis*

The full names of the sugars are as follows: GlcNAc, glucosamine; GlcNAcA, 2-acetamido-2,3-dideoxy-D-glucuronic acid; 3-keto-D-GlcNAcA, 2-acetamido-2-deoxy-D-*ribo*-hex-3-uluronic acid; GlcNAc3NA, 2-acetamido-3-amino-2,3-dideoxy-D-glucuronic acid; GlcNAc3NAcA, 2,3-diacetamido-2,3-dideoxy-D-glucuronic acid; ManNAc3NAcA, 2,3-diacetamido-2,3-dideoxy-D-mannuronic acid. The reaction step catalysed by WbpI/WlbD is shown in bold. Adapted from Miller et al. [10] and Wenzel, C. Q., Daniels, C., Keates, R. A., Brewer, D. and Lam, J. S. (2005) Evidence that WbpD is an N-acetyltransferase belonging to the hexapeptide acyltransferase superfamily and an important protein for O-antigen biosynthesis in *Pseudomonas aeruginosa* PAO1. Mol. Microbiol. **57**, 1288–1303, with permission from Blackwell Publishing Ltd.

EXPERIMENTAL

Materials

UDP-α-D-GlcNAc, glucose, $NADP^+$, sodium phosphate, potassium phosphate, sodium chloride, imidazole and ampicillin were obtained from Sigma–Aldrich. HiTrap Chelating HP columns were purchased from Amersham Biosciences. *E. coli* Rosetta™ and BL21(DE3) expression strains were from Novagen. LB (Luria–Bertani) medium and IPTG (isopropyl-thio-β-D-galactopyranoside) were from Invitrogen Life Technologies. All aqueous solutions were prepared with water purified by a Super-Q water system (Millipore).

Analytical techniques

A discontinuous SDS/PAGE system was used [13]. The separating gel contained 12.5 % acrylamide and, after electrophoretic separation, the gels were stained with 0.1 % Coomassie Brilliant Blue R-250 dissolved in 25 % ethanol and 10 % acetic acid (Sigma–Aldrich). The concentration of purified protein was determined using the Bradford assay [14].

Cloning and overexpression of His_6–WbpI and His_6–WlbD

The *wbpI* gene from *P. aeruginosa* PAO1 (serotype O5) was amplified from genomic DNA by PCR using the forward

primer 5′-CACTCT**ACATGT**CGATGAAAATTCTGACCATC-ATTG-3′, which incorporates an AflIII restriction digestion site (underlined and bold, compatible with NcoI), and reverse primer 5′-GCTCA**GGATCC**TCACAGCTTGGCAAGATATTC-3′, which incorporates a BamHI restriction digestion site (underlined and bold). Typically, PCR reactions contained 100 ng of template DNA, 0.5 μM of each primer, 2.5 mM of each dNTP, and 1× Expand Buffer 1. A 5 min denaturation at 94 °C was performed before the addition of 2.5 units of Expand Long Template Enzyme (Roche Diagnostics), followed by 20 cycles of 45 s at 94 °C, 30 s annealing at 55 °C, and 90 s elongation at 68 °C. A final 5 min elongation step at 68 °C was performed.

For protein expression, *wbpI* from *P. aeruginosa* PAO1 was cloned into the pET-23dr expression vector [15] with an N-terminal histidine tag in a two-step process. *wbpI* was amplified by Expand Long Template PCR (described above) and cloned into the vector pCR 2.1 using the TOPO TA cloning kit (Invitrogen) according to the manufacturer's protocol. The resulting construct was verified by restriction digestion. Then, the pCR 2.1-wbpI clone was digested with AflIII and BamHI, while the target vector, pET-23dr, was digested with NcoI and BamHI. The *wbpI* insert from pCR 2.1-wbpI and the linearized pET-23dr vector were purified using UltraClean™ 15 (Bio/Can Scientific) and ligated overnight at 15 °C using T4 DNA ligase (New England Biolabs). The resulting construct, pWMJL072, was verified by restriction digestion and sequencing.

Subsequently, pWMJL072 was transformed into the expression strain *E. coli* Rosetta™, using ampicillin (100 μg/ml) and chloramphenicol (34 μg/ml) for selection. For the expression of His_6–WbpI, 250 ml of LB broth containing ampicillin and chloramphenicol was inoculated with 5 ml of an overnight culture, and grown at 37 °C. When $D_{600\,nm}$ reached 0.5, the culture was transferred to 15 °C, and when the $D_{600\,nm}$ reached 0.6, IPTG was added to a final concentration of 0.1 mM. Expression was allowed to proceed overnight (about 20 h) at 15 °C. Cells were harvested by centrifugation at 10000 ***g*** for 10 min at 4 °C, and the pellets were stored at −20 °C.

The *wlbD* gene from *B. pertussis* BP536, a streptomycin-resistant derivative of strain Tohama I [16], was amplified from a boiled cell lysate by PCR using the forward primer 5′-CAC-CAC**TCATGA**CGATGCCGAAGAAGATACTGACCGTACTG-3′, which incorporates an BspHI restriction digestion site (underlined and bold, compatible with NcoI), and reverse primer 5′-GC-**GGATCC**TCAGTGGGCGGCCAGGGC-3′, which incorporates a BamHI restriction digestion site (underlined and bold). PCR reactions were set up with KOD polymerase, according to the manufacturer's protocol (Novagen). A 2 min denaturation at 94 °C was performed, followed by 25 cycles of 15 s at 94 °C, 30 s annealing at 58 °C, and 70 s elongation at 68 °C. A final 7 min elongation step at 68 °C was performed.

For protein expression, the PCR-amplified and digested *wlbD* gene was gel-extracted using a High Pure PCR Purification Kit (Roche Diagnostics), then ligated using T4 DNA ligase (Invitrogen) into the pET-23dr expression vector [15] via NcoI and BamHI restriction sites. The resulting construct, pEWJL201, was verified by restriction digestion and sequencing. Subsequently, pEWJL201 was transformed into the expression strain *E. coli* Rosetta™, using ampicillin (100 μg/ml) and chloramphenicol (34 μg/ml) for selection. Expression conditions were identical with those for His_6–WbpI.

Purification of His_6–WbpI and His_6–WlbD

The pellet from 250 ml of induced culture was resuspended in 10 ml of purification buffer [50 mM sodium phosphate (pH 7.5), 200 mM sodium chloride and 5 mM imidazole]. The cells were disrupted by ultrasonication on ice, and cell debris and membrane fractions were removed by ultracentrifugation at 49000 rev./min for 1 h at 4 °C (Type 70 Ti rotor; Beckman L8-55 M ultracentrifuge). Purification using an ÄKTA-FPLC system (Amersham Biosciences) was accomplished using a 1 ml HiTrap chelating HP column following the manufacturer's protocol, with nickel as the chelating ion. After loading the column with 10 ml of the protein sample, the column was washed with 20 column volumes of purification buffer containing 20 mM imidazole, and then with 5 column volumes of purification buffer containing 60 mM imidazole. Finally, purification buffer containing 150 mM imidazole was used as the eluent. Following purification, the buffers of the purified samples were exchanged using a PD-10 desalting column (Amersham Biosciences) according to the manufacturer's protocol. For NMR analysis, samples were exchanged into 25 mM sodium phosphate (pH 7.5) and 50 mM sodium chloride. For storage of either enzyme, samples were exchanged into 50 mM sodium phosphate (pH 7.5), 100 mM sodium chloride and 25 % glycerol. The purities of His_6–WbpI and His_6–WlbD were analysed by SDS/PAGE, and the proteins were quantified using the Bradford assay [14]. Estimation of the purity was accomplished by analysis of an overloaded SDS/PAGE gel by Quantity One™ software (Version 4.6.1, Bio-Rad Laboratories).

Determination of optimal reaction conditions using His_6–WbpI

Each reaction variable was altered in turn to identify the optimal conditions. The standard conditions for all reactions included 1 mM UDP-α-D-GlcNAc3NAcA and 0.17 mM $NADP^+$ (included as an internal standard); unless stated, reactions had a total volume of 60 μl and were incubated at 37 °C for 1.5 h. For determination of the buffer and pH optimum, reactions used 3.6 μg His_6–WbpI and were performed in 20 mM Tris-HCl buffer at pH 6.8, 7.5, 8.2 or 9.5; in 20 mM potassium phosphate buffer at pH 5.8, 6.8 or 7.8; and in 20 mM sodium phosphate buffer at pH 6.0, 7.0, 7.5 or 8.0. The temperature optimum was established by incubating reaction mixtures in 20 mM sodium phosphate buffer, pH 6.0 at 16, 30, 37 or 42 °C. For the determination of the optimal incubation time and ideal amount of enzyme, 35 μl reaction mixtures were used to conserve the substrate material. The optimal incubation time was determined for reactions set up in 20 mM sodium phosphate buffer (pH 6.0), which were allowed to proceed at 37 °C for 15 min–6 h. Finally, to determine the ideal amount of His_6–WbpI to use, reactions were set up in 20 mM sodium phosphate buffer at pH 6.0, with various amounts of His_6–WbpI. In all cases, the completed reaction mixtures were centrifuged at 13000 ***g*** for 10 min at 4 °C before loading for CE analysis. The percentage substrate conversion value for each study was determined by integrating the area under the curve obtained by CE using the Beckman 32 Karat™ Software.

Analysis of substrate specificity of His_6–WbpI and His_6–WlbD

Each reaction mixture contained 20 mM sodium phosphate (pH 6.0), 0.17 mM $NADP^+$ and 1.75 μg of purified enzyme in a total reaction volume of 35 μl. UDP-α-D-GlcNAc, UDP-α-D-GlcNAcA, UDP-α-D-GlcNAc3NAc, and UDP-α-D-GlcNAc-3NAcA were used at a final concentration of 1 mM, and reactions were incubated at 37 °C for 1.5 h or 5 h. Reactions were stopped by freezing in a dry-ice/ethanol bath, and were then centrifuged at 13000 ***g*** for 10 min at 4 °C and loaded for CE analysis.

CE analyses

CE analyses were performed using a P/ACE MDQ Glycoprotein System (Beckman Coulter) with UV detection. The running

buffer was 25 mM sodium tetraborate (unaltered pH 9.4), and the capillary was bare silica 75 μm × 50 cm with a detector at 40 cm. The capillary was conditioned before each run by washing with 1 M sodium hydroxide for 2 min, and then running buffer for 2 min. Samples were introduced by pressure injection for 8 s, in the case of 60 μl reactions, and for 16 s in the case of 35 μl reactions. The separation was performed at 22 kV and monitored by measuring UV absorbance at 254 nm. Peak integration was performed using the Beckman 32 Karat™ Software.

NMR spectroscopy

To identify the reaction product of His_6–WbpI, the enzymatic reaction was performed in the NMR tube [200 μl, 90 % H_2O/10 % ^2H_2O, 20 mM NaH_2PO_4 buffer (pH 6.4), 80 μg of His_6–WbpI, 10 mM UDP-α-D-GlcNAc3NAcA at 37 °C] and examined directly through the acquisition of a proton spectrum every 10 min (128 transients). This approach avoids the need to purify minor reaction products resulting from incomplete enzymatic reactions, which might be difficult to separate from the starting material. Proton spectra were acquired using a Varian Inova 500 MHz (^{1}H) spectrometer (Varian) with a Varian Z-gradient 3-mm triple resonance (^{1}H, ^{13}C, ^{31}P) probe. To characterize the structure of the His_6–WbpI reaction product in detail, reaction buffer was freeze-dried, exchanged into ^2H_2O (Cambridge Isotopes Laboratories) and examined using a Varian 600 MHz (^{1}H) NMR spectrometer equipped with a Varian Z-gradient 5-mm triple resonance (^{1}H, ^{13}C, ^{15}N) cryogenically cooled probe (cold probe) for optimal sensitivity. Standard homo- and hetero-nuclear correlated two-dimensional ^{1}H NMR, COSY, TOCSY, NOESY, ^{13}C HSQC (heteronuclear single-quantum coherence) and HMBC (heteronuclear multiple-bond correlation) pulse sequences from Varian were used for general assignments. Selective one-dimensional TOCSY experiments with a Z-filter and one-dimensional NOESY experiments were used for complete residue assignments and measurements of proton coupling constants ($J_{H,H}$) and nuclear Overhauser enhancements [17,18]. NMR experiments were performed with suppression of the HOD resonance at δ_H 4.78 p.p.m. and the methyl resonance of acetone was used as an internal reference (δ_H 2.225 p.p.m., δ_C 31.07 p.p.m.).

RESULTS AND DISCUSSION

Expression and purification of His_6–WbpI and His_6–WlbD

His_6–WbpI expression in *E. coli* Rosetta™ cells was effective in producing a reasonable yield of the protein. However, a large proportion of the protein was found in the pellet after the low-speed centrifugation, indicating that it had probably formed inclusion bodies. Total yield after purification and buffer exchange was about 0.5–1.5 mg of His_6–WbpI from 250 ml of culture. His_6–WbpI was purified to more than 70 % homogeneity, as judged by densitometry analysis. The apparent molecular mass of His_6–WbpI (40.3 kDa) from SDS/PAGE correlates well with the predicted molecular mass of 40.2 kDa (Figure 2).

His_6–WlbD from *E. coli* Rosetta™ cells mainly localized to the soluble fraction. A high yield of about 8–9 mg of His_6–WlbD could be achieved from 250 ml of culture. Purification by affinity chromatography produced His_6–WlbD at 98.8 % purity, as calculated from densitometry analysis. On an SDS/PAGE gel, His_6–WlbD migrates with an apparent molecular mass of 42.6 kDa, which is somewhat higher than the predicted molecular mass of 40.6 kDa (Figure 2). His_6–WbpI and His_6–WlbD enzymes stored at −20 °C in the presence of 25 % glycerol retained activity for at least 4 weeks.

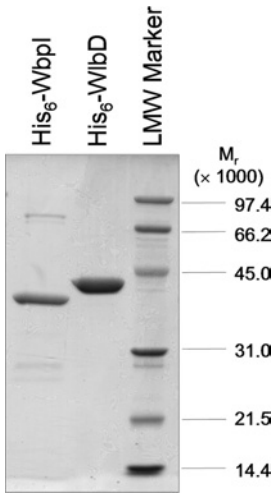

Figure 2 Purified His_6–WbpI and His_6–WlbD after nickel-affinity chromatography

Each protein was eluted at 150 mM imidizole, then exchanged into 50 mM sodium phosphate (pH 7.5), 100 mM sodium chloride and 25 % glycerol. A total of 2 μg of protein, as calculated using the Bradford assay, was loaded in each lane. LMW Marker, low molecular-mass marker.

Although the same purification conditions were used for both enzymes, His_6–WlbD is almost 40 % more pure than His_6–WbpI. This difference is ascribed to the differing solubility of the two proteins, with His_6–WbpI being found predominantly in inclusion bodies even after optimization of expression conditions. However, analysis of the reactions with His_6–WbpI showed that only one new peak was formed by incubation with enzyme, and this peak corresponded to UDP-α-D-ManNAc3NAcA (see below). The His_6–WbpI preparation described in the present study was therefore deemed suitable for our analysis since the minor contaminating proteins do not catalyse any reaction under these conditions.

Functional characterization of His_6–WbpI and His_6–WlbD using CE

CE analysis of reactions containing UDP-α-D-GlcNAc3NAcA and $NADP^+$ and catalysed by purified His_6–WbpI revealed three discrete peaks with relatively long retention times of about 12.8 min, 13.2 min and 13.8 min (Figure 3). The first and the last of the three peaks were identified as $NADP^+$ and UDP-α-D-GlcNAc3NAcA respectively, by comparison with standards and by spiking the reaction with additional material to show the increase in the peak integral. The smallest peak (at about 13.2 min), which migrated between $NADP^+$ and UDP-α-D-GlcNAc3NAcA, was not found in control reactions lacking enzyme, and was subsequently identified as UDP-α-D-ManNAc3NAcA by NMR spectroscopy (see below). An identical reaction product peak was observed when purified His_6–WlbD was used as the enzyme in the reaction (Figure 3).

Optimal reaction conditions

Initially, reactions with His_6–WbpI were arbitrarily performed in 20 mM Tris/HCl (pH 7.5). However, these reactions yielded a relatively low percentage conversion of substrate (~6 %), which was interpreted as indicating that the enzyme was not reacting under optimal conditions. The incubation time, buffer, pH and temperature optima for His_6–WbpI-catalysed reactions were therefore investigated by comparing the total percentage substrate

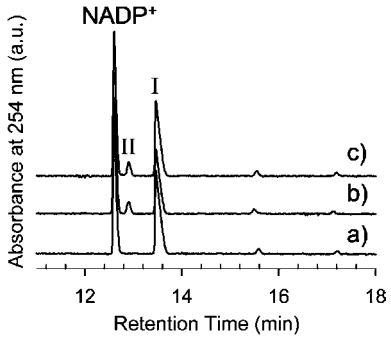

Figure 3 CE analysis of His_6–WlbD and His_6–WbpI reactions

Each reaction mixture contained 1 mM UDP-α-D-GlcNAc3NAcA (**I**) and 0.17 mM $NADP^+$ and was incubated at 37 °C for 1.5 h. (**a**) Control reaction with no enzyme. (**b**) Reaction with 0.05 mg/ml of purified His_6–WlbD. (**c**) Reaction with 0.05 mg/ml of purified His_6–WbpI. Both His_6–WbpI and His_6–WlbD reactions yielded a novel peak (**II**).

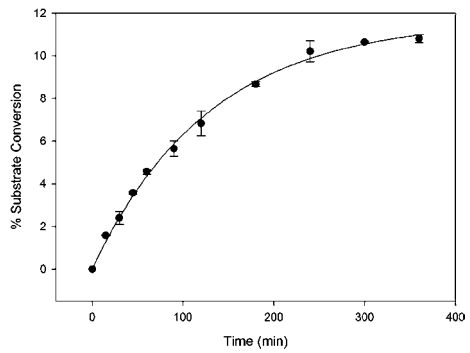

Figure 4 Time course for His_6–WbpI-catalysed reactions after incubation at 37 °C

All reactions contained 20 mM sodium phosphate (pH 6.0), 0.17 mM $NADP^+$, 1 mM UDP-α-D-GlcNAc3NAcA and 0.06 mg/ml of His_6–WbpI. Each data point represents the mean ± S.D. of the mean determined from two experiments performed in duplicate.

conversion into product under various conditions. Of the incubation times tested, 4 h was determined to be the time when the epimerization reaction had reached equilibrium at approximately 10 % substrate conversion when 0.06 mg/ml of enzyme and 1 mM substrate was used. Further incubation of the reaction mixture did not significantly change the value of percentage conversion of substrate into product (Figure 4). Addition of extra enzyme after incubation for 6 h did not cause additional conversion of substrate into product, which indicated that the apparent equilibrium was not due to enzyme inactivation under the experimental conditions (results not shown). Various buffers, including Tris/HCl, potassium phosphate and sodium phosphate were tested over a range of pH values within their respective ranges of good buffering. Improved substrate conversion was shown in all three buffer systems when more acidic pH conditions were used, and sodium phosphate (pH 6.0), yielded the highest percentage substrate conversion (results not shown). The temperature optimum for His_6–WbpI-catalysed reactions was investigated, and incubation at 30–37 °C gave the highest percentage substrate conversion (results not shown). Several different quantities of enzyme were reacted with a constant amount of substrate (1 mM) and this indicated that 0.2 μg of His_6–WbpI in a 35 μl reaction volume was sufficient to yield an observable conversion (> 1 %) of substrate into product in 1.5 h at 37 °C (results not shown). After all of the reaction parameters were optimized, an approximately 2-fold improvement in the percentage conversion was observed. The final reaction conditions [20 mM sodium phosphate buffer (pH 6.0), 1 mM UDP-α-D-GlcNAc3NAcA, 1.75 μg of purified enzyme in a total reaction volume of 35 μl, incubation for 1.5 h at 37 °C] were used for both His_6–WbpI and His_6–WlbD in subsequent analyses.

Substrate specificity of His_6–WbpI and His_6–WlbD

Reactions with His_6–WbpI or His_6–WlbD were set up, in which various possible substrates including UDP-α-D-GlcNAc, UDP-α-D-GlcNAcA, UDP-α-D-GlcNAc3NAc, and UDP-α-D-GlcNAc3NAcA were used at a final concentration of 1 mM. A product peak was observed only when UDP-α-D-GlcNAc3NAcA was used as the substrate for reaction with either His_6–WbpI or His_6–WlbD (results not shown). When potential substrates, including UDP-α-D-GlcNAc, UDP-α-D-GlcNAcA or UDP-α-D-GlcNAc3NAc, which share structural features with the proposed substrate, UDP-α-D-GlcNAc3NAcA, were provided in His_6–WbpI or His_6–WlbD reactions, no conversion of substrate into product could be discerned. In contrast, up to 13 % of the UDP-α-D-GlcNAc3NAcA was converted into product, showing that His_6–WbpI and His_6–WlbD are highly discriminatory towards their substrate. This clearly demonstrates that His_6–WbpI and His_6–WlbD specifically act on UDP-α-D-GlcNAc3NAcA.

Investigation of the His_6–WbpI reaction directly in the NMR tube

^1H NMR can be used as a real-time analytical probe to continuously and directly follow enzymatic reactions in the NMR tube [19–21]. Using this approach, we examined the His_6–WbpI reaction (Figure 5) and were able to identify the minor reaction products in the presence of the starting material, since the reactions never went to completion. Within the first few minutes of the His_6–WbpI reaction, we observed a decrease in the anomeric signal for the UDP-α-D-GlcNAc3NAcA (**I**) substrate at δ_H 5.55 p.p.m. and the appearance of a novel anomeric signal (**II**) at δ_H 5.46 p.p.m. (Figures 5a and 5b). A minor impurity was also observed at δ_H 5.40 p.p.m. (*) and was determined to originate from the chemically synthesized starting material. Equilibrium was reached in the His_6–WbpI reaction after 85 min and resulted in approximately 19 % conversion of **I** into **II** (Figure 5c). Examination of the kinetics of substrate conversion into product by His_6–WbpI in the in-tube NMR approach revealed that the rate of loss of the substrate was equal to the rate of gain of the product. This suggests that His_6–WbpI does not exhibit any activity for UDP-α-D-GlcNAc3NAcA other than C2 epimerization under the conditions used for analysis [20 mM sodium phosphate (pH 6.0), 37 °C, 1 mM substrate]. Study of the reaction kinetics of WbpI in the conventional manner, to determine K_m and k_{cat}, were not attempted due to the limited amount of the chemically synthesized substrate, UDP-α-D-GlcNAc3NAcA, that is currently available. Therefore detailed kinetic studies are required into the enzymes upstream in this pathway that allow the enzymatic synthesis of UDP-α-D-GlcNAc3NAcA, as well as a strategy to improve the sensitivity of detecting UDP-α-D-ManNAc3NAcA in reaction mixtures.

Identification of the His_6–WbpI reaction product by NMR spectroscopy

To identify the reaction products unambiguously, the aqueous reaction buffer from the His_6–WbpI reaction was freeze-dried after the concentration of UDP-α-D-ManNAc3NAcA (**II**) was maximal, exchanged into ^2H_2O and examined with NMR using a combination of one- and two-dimensional experiments. The

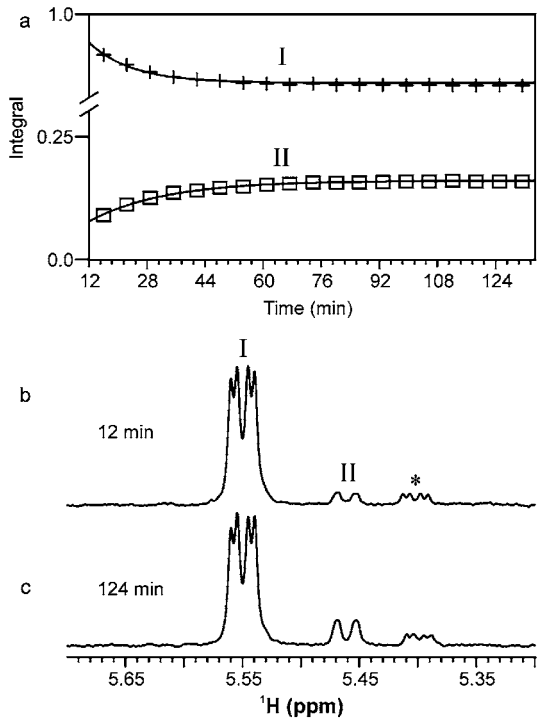

Figure 5 The WbpI reaction performed in an NMR tube and examined directly with NMR spectroscopy at 500 MHz (^{1}H)

The reaction mixture contained 90% H_2O/10% ^2H_2O, 20 mM sodium phosphate (pH 6.4), 80 μg of His_6–WbpI, 10 mM UDP-α-D-GlcNAc3NAcA in 200 μl, and was incubated at 37 °C. (**a**) A plot showing the progress of the His_6–WbpI reaction that converts UDP-α-D-GlcNAc3NAcA (**I**) into UDP-α-D-ManNAc3NAcA (**II**) expressed as integrals for anomeric signals compared with time (integrals are normalized to **I**). The reaction was monitored directly through the acquisition of a proton spectrum at 10 min intervals (128 transients). (**b**) and (**c**) Proton spectra for the WbpI reaction showing the anomeric region at 12 min and 124 min respectively. * Represents a minor impurity that was present in the chemically synthesized substrate.

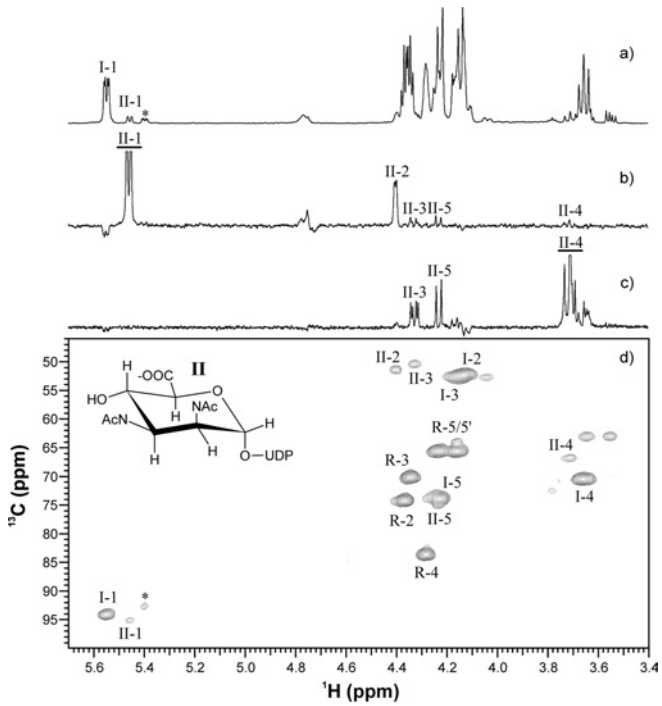

Figure 6 NMR spectroscopy of the WbpI reaction product UDP-α-D-ManNAc3NAcA (II)

(**a**) Proton spectrum (64 transients). (**b**) One-dimensional TOCSY (150 ms) of **II** H1. (**c**) One-dimensional TOCSY (80 ms) of **II** H4. (**d**) ^{13}C HSQC spectrum (384 transients, 128 increments, $^1J_{C,H} = 146$, 7 h). **I** represents UDP-α-D-GlcNAc3NAcA, R represents ribose and * represents a minor impurity that was present in the chemically synthesized substrate. For selective one-dimensional experiments, excited resonances are underlined.

proton spectrum of the His_6–WbpI reaction revealed three sets of anomeric signals: those at δ_H 5.55 p.p.m. corresponding to the UDP-α-D-GlcNAc3NAcA (**I**) substrate (Table 1), another at δ_H 5.46 p.p.m. corresponding to the reaction product (**II**), and a minor signal at δ_H 5.40 p.p.m. which originated from an unknown impurity (*) (Figure 6a). Selective one-dimensional TOCSY experiments were used to assign proton resonances and measure coupling constants for **II**. One-dimensional TOCSY of **II** H1 (150 ms) revealed several *J*-coupled resonances corresponding to H2, H3, H4 and H5 (Figure 6b), while that of H4 (80 ms) revealed signals for H3 and H5 (Figure 6c). Small $J_{1,2}$ and $J_{2,3}$, large $J_{3,4}$ (10.7 Hz) and $J_{4,5}$ (10.1 Hz) coupling constants, and the doublet for the H5 resonance indicated a mannuronic acid [22–24]. Carbon assignments were made based on proton–carbon correlations observed using a ^{13}C HSQC experiment (Figure 6d) and assignments for carbon atoms without protons were made using an HMBC experiment (results not shown). Carbon chemical shifts for **II** were found to be in good agreement with those reported for ManNAc3NAcA [22,23,25]. A two-dimensional

Table 1 NMR data for the His_6–WbpI (*P. aeruginosa*) reaction

NMR spectra referenced to an internal acetone standard (δ_H 2.225 p.p.m., δ_C 31.07 p.p.m.).

		^{1}H and ^{13}C chemical shifts (δ p.p.m.) and proton coupling constants ($J_{H,H}$ Hz)									
		H1	H2	H3	H4	H5	H6	NAc-CH_3	NAc-CO	NAc-CH_3	NAc-CO
		C1	C2	C3	C4	C5	C6				
Compound		$J_{1,2}$	$J_{2,3}$	$J_{3,4}$	$J_{4,5}$	$J_{5,6}$					
UDP-α-D-GlcNAc3NAcA	δ_H	5.55	4.12	4.15	3.66	4.23	1.99	2.01			
	δ_C	94.2	52.3	52.6	70.5	74.0	176.9	22.7	175.6	22.7	175.3
	$J_{H,H}$	2.8	11.2	11.3	10.1						
	$J_{P,H}$	7.4									
UDP-α-D-ManNAc3NAcA	δ_H	5.46	4.40	4.33	3.71	4.23	1.95	2.04			
	δ_C	95.1	51.5	50.5	66.9	75.0	176.9	22.7	175.3	22.7	175.1
	$J_{H,H}$	1.5	4.1	10.7	10.1						
	$J_{P,H}$	8.0									

NOESY experiment (800 ms, results not shown) revealed an NOE (nuclear Overhauser effect) between H3-H5 of **II** and no NOE between H2–H4 thereby confirming the identity of the His_6–WbpI reaction product **II** as UDP-α-D-ManNAc3NAcA. CE had previously shown that the product of His_6–WlbD is identical with that of His_6–WbpI, so the NMR results suggest that both His_6–WbpI and His_6–WlbD are UDP-α-D-GlcNAc3NAcA 2-epimerases.

Potential reaction mechanism of UDP-α-D-GlcNAc3NAcA 2-epimerases

Previous work on UDP-α-D-GlcNAc 2-epimerase from *E. coli* (RffE) established that the reaction proceeds through a glycal mechanism involving 'anti' elimination and 'syn' addition, which results in the production of 2-acetamidoglucal and UDP as reaction intermediates that are normally retained by the enzyme but released once every 1000 turnovers [26]. The structure of RffE bound to UDP has been determined, and the identities of several amino acids important for binding UDP or recognizing the sugar moiety of the substrate were proposed [27]. As observed by Field and Naismith [28], all of the important residues of RffE are conserved in WbpI and WlbD, with one exception. The structure of WlbD has previously been investigated, and the residues proposed to be involved in UDP and sugar binding were found to be placed in appropriate regions to allow for a mechanism like that used by RffE [28,29]. Additionally, comparison of the RffE and WlbD structures showed a root mean square deviation of 1.03 Å (1 Å = 0.1 nm), calculated over 120 α-carbon atoms from WlbD that are conserved in RffE [28]. Thus it is fascinating that RffE and WlbD may have not only the same residues involved in binding UDP, but the same residues involved in binding GlcNAc or GlcNAc3NAcA respectively. The one residue that is altered in WlbD and WbpI relative to RffE is Phe^{276}, which is a methionine residue in both WbpI and WlbD. This residue is proposed to play a role in stabilizing the bound UDP by π-stacking of the uracil ring between Phe^{276} and Arg^{10} [27], but this does not explain the different substrate specificities of RffE compared with WlbD and WbpI. Further investigation of the mechanism of catalysis in WbpI and WlbD is currently in progress, employing site-directed mutagenesis to probe the importance of key residues in WbpI and WlbD. An intriguing note is that the production of UDP as a reaction intermediate should have been detected if WbpI and WlbD were using an RffE-like mechanism. However, even after 6 h in a time-course experiment, no UDP could be discerned.

In summary, in the present study, we have shown that His_6–WbpI and His_6–WlbD were purified to ~70 % and ~90 % purity respectively, using FPLC and affinity chromatography. Optimal reaction conditions for His_6–WbpI were established, and used to improve the percentage substrate conversion achieved in both His_6–WbpI- and His_6–WlbD-catalysed reactions. Although a set of potential substrates were tested, both enzymes exhibited activity only with the proposed substrate, UDP-α-D-GlcNAc3NAcA. The approach of performing NMR analysis of in-tube reactions allowed the progress of the His_6–WbpI-catalysed reactions to be observed directly in aqueous reaction buffer. This has helped to avoid the need to separate the product from the substrate and to concentrate the purified product by freeze-drying. Since many sugar–nucleotide intermediates or products are labile and could not remain intact during such purification steps, the in-tube NMR reaction vastly accelerated the analysis. The identity of the His_6–WbpI reaction product was unambiguously determined to be UDP-α-D-ManNAc3NAcA by NMR spectroscopy, which demonstrated that WbpI is a UDP-α-D-GlcNAc3NAcA 2-epimerase. The product produced by His_6–WlbD is identical with that of His_6–WbpI, as judged by CE analysis. Thus both His_6–WbpI and His_6–WlbD are involved in the production of UDP-α-D-ManNAc3NAcA, a component of the B-band LPS in *P. aeruginosa* serotype O5 and the band-A trisaccharide of *B. pertussis, Bordetella parapertussis* and *Bordetella bronchiseptica*. Although several 2-epimerases have been characterized, this is the first report of the expression, purification and biochemical characterization of two novel proteins of the 2-epimerase family that are specific for UDP-α-D-GlcNAc3NAcA as a substrate. Based on the biochemical data obtained in the present study, WbpI and WlbD should be properly named UDP-2,3-diacetamido-2,3-dideoxy-α-D-glucuronic acid 2-epimerases, and be assigned the enzyme classification EC 5.1.3 (Isomerases: Racemases and epimerases: acting on carbohydrates and derivatives).

This work was supported by a grant from CIHR (Canadian Institutes of Helath Research; MOP#. 14687) to J.S.L., and grants to R.A.F. from the BBSRC (Biotechnology and Biological Sciences Research Council) and EPSRC (Engineering and Physical Sciences Research Council). A.P. was supported by an NSERC (National Science and Engineering Research Council of Canada) Discovery Grant. D.J.McN. was supported by a Wellcome Trust Programme (Grant # 054588). J.-R.B. and D.J.McN. are supported by the NRC-IBS (National Research Council Canada, Institute for Biological Sciences) Research program. E.L.W. was a recipient of an NSERC PGS-D [Postgraduate Scholarship (Doctoral)] and currently holds a CIHR CGS-D [Canada Graduate Scholarship (Doctoral)]. W.L.M. was a recipient of a CIHR DRA. J.S.L. holds a Canada Research Chair in Cystic Fibrosis and Microbial Glycobiology.

REFERENCES

1 Harvill, E. T., Preston, A., Cotter, P. A., Allen, A. G., Maskell, D. J. and Miller, J. F. (2000) Multiple roles for *Bordetella* lipopolysaccharide molecules during respiratory tract infection. Infect. Immun. **68**, 6720–6728
2 Dasgupta, T., de Kievit, T. R., Masoud, H., Altman, E., Richards, J. C., Sadovskaya, I., Speert, D. P. and Lam, J. S. (1994) Characterization of lipopolysaccharide-deficient mutants of *Pseudomonas aeruginosa* derived from serotypes O3, O5, and O6. Infect. Immun. **62**, 809–817
3 Engels, W., Endert, J., Kamps, M. A. and van Boven, C. P. (1985) Role of lipopolysaccharide in opsonization and phagocytosis of *Pseudomonas aeruginosa*. Infect. Immun. **49**, 182–189
4 Meier-Dieter, U., Starman, R., Barr, K., Mayer, H. and Rick, P. D. (1990) Biosynthesis of enterobacterial common antigen in *Escherichia coli*. Biochemical characterization of Tn10 insertion mutants defective in enterobacterial common antigen synthesis. J. Biol. Chem. **265**, 13490–13497
5 Kiser, K. B., Bhasin, N., Deng, L. and Lee, J. C. (1999) *Staphylococcus aureus* cap5P encodes a UDP-*N*-acetylglucosamine 2-epimerase with functional redundancy. J. Bacteriol. **181**, 4818–4824
6 Portoles, M., Kiser, K. B., Bhasin, N., Chan, K. H. and Lee, J. C. (2001) *Staphylococcus aureus* Cap5O has UDP-ManNAc dehydrogenase activity and is essential for capsule expression. Infect. Immun. **69**, 917–923
7 Burrows, L. L., Charter, D. F. and Lam, J. S. (1996) Molecular characterization of the *Pseudomonas aeruginosa* serotype O5 (PAO1) B-band lipopolysaccharide gene cluster. Mol. Microbiol. **22**, 481–495
8 Wenzel, C. Q., Daniels, C., Keates, R. A., Brewer, D. and Lam, J. S. (2005) Evidence that WbpD is an N-acetyltransferase belonging to the hexapeptide acyltransferase superfamily and an important protein for O-antigen biosynthesis in *Pseudomonas aeruginosa* PAO1. Mol. Microbiol. **57**, 1288–1303
9 Burrows, L. L., Pigeon, K. E. and Lam, J. S. (2000) *Pseudomonas aeruginosa* B-band lipopolysaccharide genes wbpA and wbpI and their *Escherichia coli* homologues wecC and wecB are not functionally interchangeable. FEMS Microbiol. Lett. **189**, 135–141
10 Miller, W. L., Wenzel, C. Q., Daniels, C., Larocque, S., Brisson, J. R. and Lam, J. S. (2004) Biochemical characterization of WbpA, a UDP-*N*-acetyl-D-glucosamine 6-dehydrogenase involved in O-antigen biosynthesis in *Pseudomonas aeruginosa* PAO1. J. Biol. Chem. **279**, 37551–37558
11 Allen, A. and Maskell, D. (1996) The identification, cloning and mutagenesis of a genetic locus required for lipopolysaccharide biosynthesis in *Bordetella pertussis*. Mol. Microbiol. **19**, 37–52
12 Preston, A., Thomas, R. and Maskell, D. J. (2002) Mutational analysis of the *Bordetella pertussis* wlb LPS biosynthesis locus. Microb. Pathog. **33**, 91–95

13 Laemmli, U. K. (1970) Cleavage of structural proteins during the assembly of the head of bacteriophage T4. Nature **227**, 680–685
14 Bradford, M. M. (1976) A rapid and sensitive method for the quantitation of microgram quantities of protein utilizing the principle of protein-dye binding. Anal. Biochem. **72**, 248–254
15 Newton, D. T. and Mangroo, D. (1999) Mapping the active site of the *Haemophilus influenzae* methionyl-tRNA formyltransferase: residues important for catalysis and tRNA binding. Biochem. J. **339**, 63–69
16 Relman, D., Tuomanen, E., Falkow, S., Golenbock, D. T., Saukkonen, K. and Wright, S. D. (1990) Recognition of a bacterial adhesion by an integrin: macrophage CR3 (αMβ2, CD11b/CD18) binds filamentous hemagglutinin of *Bordetella pertussis*. Cell **61**, 1375–1382
17 Brisson, J. R., Sue, S. C., Wu, W. G., McManus, G., Nghia, P. T. and Uhrin, D. (2002) In NMR Spectroscopy of Glycoconjugates (Jimenez-Barbero, J. and Peters, T., eds.), pp. 59–93, Wiley-VCH, Weinhem, Germany
18 Uhrin, D. and Brisson, J. R. (2000) In NMR in Microbiology: Theory and Applications (Barbotin, J. N. and Portais, J. C., eds.), pp. 165–190, Horizon Scientific Press, Wymondham, U.K.
19 Pfoestl, A., Hofinger, A., Kosma, P. and Messner, P. (2003) Biosynthesis of dTDP-3-acetamido-3,6-dideoxy-α-D-galactose in *Aneurinibacillus thermoaerophilus* L420-91T. J. Biol. Chem. **278**, 26410–26417
20 Pellecchia, M. (2005) Solution nuclear magnetic resonance spectroscopy techniques for probing intermolecular interactions. Chem. Biol. **12**, 961–971
21 McNally, D. J., Schoenhofen, I. C., Mulrooney, E. F., Whitfield, D. M., Vinogradov, E., Lam, J. S., Logan, S. M. and Brisson, J. R. (2006) Identification of labile UDP-ketosugars in *Helicobacter pylori*, *Campylobacter jejuni* and *Pseudomonas aeruginosa*: key metabolites used to make glycan virulence factors. Chembiochem. **7**, 1865–1868
22 Knirel, Y. A., Vinogradov, E. V., Shashkov, A. S., Dmitriev, B. A., Kochetkov, N. K., Stanislavsky, E. S. and Mashilova, G. M. (1982) Somatic antigens of *Pseudomonas aeruginosa*. the structure of O-specific polysaccharide chains of *P. aeruginosa* O:3a, b and O:3a, d lipopolysaccharides. Eur. J. Biochem. **128**, 81–90
23 Knirel, Y. A., Paramonov, N. A., Vinogradov, E. V., Shashkov, A. S., Dmitriev, B. A., Kochetkov, N. K., Kholodkova, E. V. and Stanislavsky, E. S. (1987) Somatic antigens of *Pseudomonas aeruginosa*. The structure of O-specific polysaccharide chains of lipopolysaccharides of *P. aeruginosa* O3 (Lanyi), O25 (Wokatsch) and Fisher immunotypes 3 and 7. Eur. J. Biochem. **167**, 549–561
24 Sadovskaya, I., Brisson, J. R., Altman, E. and Mutharia, L. M. (1996) Structural studies of the lipopolysaccharide O-antigen and capsular polysaccharide of *Vibrio anguillarum* serotype O:2. Carbohydr. Res. **283**, 111–127
25 Knirel, Y. A., Vinogradov, E. V., Shashkov, A. A., Dmitriev, B. A., Kochetkov, N. K., Stanislavsky, E. S. and Mashilova, G. M. (1983) Somatic antigens of *Pseudomonas aeruginosa*. The structure of O-specific polysaccharide chains of *P. aeruginosa* O:3(a),c and O:3a,d,e lipopolysaccharides. Eur. J. Biochem. **134**, 289–297
26 Morgan, P. M., Sala, R. F. and Tanner, M. E. (1997) Eliminations in the reactions catalyzed by UDP-*N*-acetylglucosamine 2-epimerase. J. Am. Chem. Soc. **119**, 10269–10277
27 Campbell, R. E., Mosimann, S. C., Tanner, M. E. and Strynadka, N. C. (2000) The structure of UDP-*N*-acetylglucosamine 2-epimerase reveals homology to phosphoglycosyl transferases. Biochemistry **39**, 14993–15001
28 Field, R. A. and Naismith, J. H. (2003) Structural and mechanistic basis of bacterial sugar nucleotide-modifying enzymes. Biochemistry **42**, 7637–7647
29 Sri Kannathasan, V., Staines, A. G., Dong, C. J., Field, R. A., Preston, A. G., Maskell, D. J. and Naismith, J. H. (2001) Overexpression, purification, crystallization and data collection on the *Bordetella pertussis* wlbD gene product, a putative UDP-GlcNAc 2′-epimerase. Acta Crystallogr. Sect. D Biol. Crystallogr. **57**, 1310–1312

Received 2 January 2007/15 February 2007; accepted 19 February 2007
Published as BJ Immediate Publication 19 February 2007, doi:10.1042/BJ20070017